SUPPLEMENTAL MATERIAL

Matrix mechanotransduction mediated by thrombospondin-1/integrin/YAP signaling pathway in remodeling of vessel wall

Authors: Yoshito Yamashiro, Ph.D., Bui Quoc Thang, M.D., Ph.D., Karina Ramirez, Seung Jae Shin, Tomohiro Kohata, Shigeaki Ohata, Tram Anh Vu Nguyen, Sumio Ohtsuki, Ph.D., Kazuaki Nagayama, Ph.D., and Hiromi Yanagisawa, M.D., Ph.D.

Detailed Methods

Cell culture and reagents. Rat vascular SMCs (Lonza, R-ASM-580, isolated from the aorta of 150-200 grams adult male Sprague-Dawley rats), were grown in DMEM with 20% (v/v) fetal bovine serum and 1 x Antibiotic-Antimycotic (Thermo Fisher Scientific). HUVECs were grown in HuMedia-MvG (KURABO) supplemented with 5% (v/v) fetal bovine serum and growth factors. The cell lines were used between passage 7 and 12 and tested for mycoplasma contamination using Mycoplasma detection set (TaKaRa, #6601) following the manufacture's protocol (result provided in Online Fig. XIX). Brefeldin A (B5936) was purchased from Sigma-Aldrich. PF-00562271, FAK inhibitor (S2672) was purchased from Selleck. Cytochalasin D (037-17561) and Latrunculin A (125-04363) were purchased from Wako. Jasplakinolide (AG-CN2-0037-C050) was purchased from AdipoGen Life Sciences. Recombinant human thrombospondin-1 was purchased from R&D Systems (3074-TH-050).

Plasmid. GFP-Grp1-PH plasmids were provided by T. Ijyuin (Kobe University, Japan)[1]. Myc-tagged plasmids encoding mouse Rap2A(WT), Rap2A(G12V), and Rap2A(S17N) were kindly donated by K. Kariya (Ryukyu University, Japan)[2]. YFP-Ssh1 was donated by K. Mizuno (Tohoku university, Japan)[3].

In vitro mechanical stretch. Cyclic stretch was performed using a uniaxial cell stretch system (Central Workshop Tsukuba University) following 24 h of serum starvation as described previously[4]. Rat vascular SMCs or HUVECs were plated (3×10^4 cells) on silicon elastomer bottomed culture plates (SC4Ha, Menicon Life Science) coated with cell attachment factor, containing gelatin (S006100, Thermo Fisher Scientific) and subjected to cyclic stretch with a frequency of 1.0 Hz (60 cycles/min) and 20% strain for the indicated time.

siRNA Transfection. Rat vascular SMCs were transiently transfected with 10 pmol for a final concentration of scramble (non-target) siRNA (Invitrogen, #12935110), *Itgav* siRNA (RSS310692), *Itgb1* siRNA (RSS302262), *Itgb3* siRNA (RSS308076) and *Fn1* siRNA (RSS303981) using RNAiMAX transfection reagent (Thermo Fisher Scientific) according to the manufacturer's instruction. All siRNAs were predesigned and purchased from Thermo Fisher Scientific. Cyclic stretch was performed 2 days after transfection.

Western blot analysis. Rat vascular SMCs or HUVECs were dissolved in RIPA lysis buffer (Sigma) containing 1% protease inhibitor (Wako) and 1% phosphatase inhibitor (Wako). The lysates were mixed with $3 \times$ SDS sample buffer with 2-mercaptoethanol (Wako) and boiled at 95 °C for 5 min, and then were subjected to SDS-PAGE. Proteins were transferred to a PVDF membrane (Millipore) and immunoblotted with antibodies indicated in Online Table I. Membranes were then incubated with respective anti-mouse or anti-rabbit HRP-conjugated secondary antibody (1:1000, Bio-Rad) and visualized with a chemoluminescence kit (Santa Cruz Biotechnology) or SuperSignal West Femto Maximum Sensitivity Substrate (Thermo Fisher Scientific).

Quantitative Polymerase chain reaction (PCR). RNA was isolated from rat vascular SMCs using RNeasy Plus Micro Kit (QIAGEN) and 1 µg of total RNA was subjected to reverse transcription reactions using iScript™ Reverse Transcription Supermix (Bio-Rad). SYBR Green was used for Amplicon detection and gene expression was normalized to the expression of housekeeping genes Glyceraldehyde 3-phosphate dehydrogenase (GAPDH). PCR reactions were carried out in triplicate in a CFX96 real-time PCR detection system (Bio-Rad) with one cycle of 3 min at 95 °C, then 39 cycles of 10 sec at 95 °C and 30 sec at 55 °C. Levels of mRNA were determined using the ddCt method and expressed relative to the mean dCt of controls. Primer sequences are provided in Online Table II.

Immunostaining. Rat SMCs or HUVECs, were fixed with 4% paraformaldehyde for 30 min, blocked in 5% BSA containing 0.1% Tween-20 for 1 h at 37 °C. Aortas and carotid artery were harvested and embedded in OCT (SAKURA Finetek USA Inc.) and snap frozen in liquid nitrogen. Cross sections of the mouse aortas or carotid arteries were immediately fixed with 4% paraformaldehyde for 30 min, blocked in 5% normal serum in which secondary antibody was raised, containing 0.1% Tween-20 for 1 h at 37 °C. The primary antibodies used are shown in Online Table I. Incubation was performed overnight at 4 °C. After washing, highly cross-absorbed Alexa 488, Alexa 546 or Alexa 647-conjugated secondary antibodies (Invitrogen) were added at a dilution of 1:200 for 2 h at 37 °C. Control experiments were performed by omitting the primary antibody. Slides were covered with Vectashield containing DAPI (Vector Laboratories) and viewed under a LSM 710 (ZEISS). Colocalization was measured on a single confocal section using the Colocalization-module of Imaris 9.2.1, 64-bit version (Bitplane AG).

Proximity ligation assay (PLA). Duolink™ PLA (Sigma-Aldrich) was performed following the manufacturer's instruction. The primary antibodies used are shown in Online Table I. Alexa 488-phalloidin (Invitrogen) was added to visualize actin fibers. Incubations were performed overnight at 4 °C. After washing, the PLA probes; Duolink In Situ PLA probe Anti-Mouse PLUS (DUO92001) and Duolink In Situ PLA probe Anti-Goat MINUS (DUO92006) were added for 2 h at 37 °C. Duolink In Situ Detection Reagents Orange (Invitrogen) was used for detection. Slides were covered with Duolink In Situ Mounting Medium containing DAPI (DUO82040) and viewed under a LSM 710 (ZEISS).

Immunoprecipitation. Immunoprecipitation was conducted using a Pierce Crosslink IP kit (Thermo Fisher Scientific). Antibodies against Thbs1 (A6.1 MS-421 and A4.1 MS-418, Neomarkers) or mouse normal IgG (10400C, Invitrogen) were crosslinked to protein A/G agarose beads and then incubated with protein lysates overnight at 4 °C. After washing and elution, input and IP products were analyzed using Western blotting.

Rap2 activation assay. Rap2 activation assay was performed according to the manufacture's instruction (Cell Biolabs, STA-406-2) and previous studies[5, 6]. After cyclic stretch or static condition, CTRL and *Thbs1KO* rat vascular SMCs were lysed at 4 °C by Assay/lysis buffer containing 125 mM HEPES (pH7.5), 750 mM NaCl, 5% NP-40, 50 mM $MgCl_2$, 5 mM EDTA, 10% Glycerol and active Rap2 was pulled down from lysates using agarose beads conjugated to Ral-GDS-RBD and detected by Western blotting using mouse anti-Rap2 antibodies.

Generation of Thbs1 knockout cell line. CRISPR-Cas9 plasmid, pSpCas9(BB)-2A-GFP (px458, #48138) was purchased from Addgene. The CRISPR design tool (http://crispr.mit.edu) was used to identify candidate sgRNA sequences of *Thbs1* gene. sgRNA sequence was PCR amplified and ligated into *Bbs*I site of px458. After transformation into *E.Coli,* the plasmid DNA was purified by using Midi prep kit (QIAGEN, Chatsworth, CA). Rat SMCs (1×10^5 cells) were plated in a 24-well plate and transfected with px458_sgRNA plasmid. Forty-eight h after transfection, FACS (BD FACSAria™ II, BD) was performed to isolate GFP-positive cells. Following isolation, cells were plated in a 96-well plate by limiting dilution for a single-cell cloning. Gene mutations were confirmed using Sanger sequencing (3130xl Genetic Analyzer, Applied Biosystems).

Secretome Analysis. Rat vascular SMCs were plated (3×10^4 cells) on silicon elastomer bottomed culture plates (SC4Ha, Menicon Life Science) coated with cell attachment factor (Thermo Fisher Scientific). Following 24 h of serum starvation, cyclic stretch was performed (1.0 Hz, 20% strain) for 20 h with or without 1 μM BFA. Four mL of conditioned media (CM) was collected and concentrated to 300 μl using Amicon Ultra-3K (Millipore, UFC200324), from which 200 μl was enriched with acetone precipitation and the rest was used for Silver staining. The CM were diluted 4-fold with acetone and stored at -80 °C for 1 h followed by centrifugation at 20,400 × g for 20 min at 4 °C. After centrifugation, the supernatant was removed. Pellets were resolved in 50 μl of 100 mM Tris-HCl (pH 9.0) containing 12 mM sodium deoxycholate and 12 mM N-lauroylsarcosinate. The experiments were performed three times to prepare for proteomics (n=3).

Sample preparation for proteomics The trypsin digestion was performed as described in a previously published study[7]. The samples were heated at 95 °C for 5 min and sonicated for 20 min, then reduced with 10 mM dithiothreitol at room temperature (RT) for 1 hour and alkylated with 55 mM iodoacetamide in the dark at RT for 1 h. The samples were diluted 5-fold with 50 mM ammonium bicarbonate and digested with lysyl endopeptidase at an enzyme/substrate ratio of 1:100 at RT for 3 h. Subsequently, the samples were digested with sequence-grade modified trypsin at an enzyme/substrate ratio of 1:100 at 37 °C for 16 h. Then, an equal volume of ethyl acetate was added to the sample and the mixture was acidified with trifluoroacetic acid (TFA) at a final concentration of 0.5%. The mixtures were centrifuged at 15,000 rpm for 2 min. The aqueous phases were dried up using a centrifugal evaporator (TOMY, Tokyo, Japan), and tryptic peptides were dissolved in 5% (v/v) acetonitrile with

0.1% TFA (v/v). The peptide samples were desalted with GL-Tip SDB and GL-Tip GC (GL Sciences). The eluents were dried up using a centrifugal evaporator and dissolved with 0.1% TFA for LC-MS/MS analysis.

Nano LC-ESI-MS/MS analysis for global proteomics Samples were injected into Nano-LC system coupled with Triple TOF 5600 mass spectrometer (SCIEX, USA). Peptides were loaded onto 100 µm internal diameter x 20 mm length PepMap 100 precolumn (Thermo Fisher Scientific, USA) at 5 µl/min and separated by 75 µm internal diameter × 250 mm length PepMap RSLC column (Thermo Fisher Scientific, USA) packed with 2 µm C18 beads with 100 Å pores. The flow rate was 300 nL/min with a 107 min gradient of solvent B (100% acetonitrile and 0.1% formic acid) for separation on the reversed-phase column. The injected peptides were eluted with solvent A (0.1% formic acid in Milli-Q water) and solvent B. The gradient condition was set 2% B (0–3 min), changed to 2-25% B (3-63 min), increased to 25-50% B (63-78 min), maintained 98% B (80-85 min). Data acquisition was controlled using Analyst TF1.6 software (SCIEX, USA). For Information Dependent Acquisition (IDA), precursor ions were scanned from 300 to 1250, and product ions were scanned from 100 to 1600 with an accumulation time of 50 msec. The peptides were identified using ProteinPilot 4.5 (Sciex). For protein quantification, data was acquired with data independent acquisition mode (SWATH-MS) with valuable window for precursor ions. The acquired data was analyzed using PeakView Software version 2.1 (Sciex).

Atomic Force Microscopy (AFM). AFM measurements were performed using a NanoWizard IV AFM (JPK Instruments-AG, Germany) mounted on top of an inverted optical microscope (IX73, Olympus, Japan) equipped with a digital CMOS camera (Zyla, Andor) as previously described[8]. The AFM quantitative imaging (QI) mode was then used to obtain a force-displacement curve at each pixel of 128 × 128 pixels (100 µm × 100 µm of measured area), using a precisely controlled high-speed indentation test using rectangular-shaped silicon nitride cantilevers with a cone probe (BioLever-mini, BL-AC40TS-C2, Olympus, Japan) at a spring constant of 0.08–0.10 N/m. The QI mode measurements were performed within 1 h after the transfer of the specimen cells to the AFM at room temperature RT (25 °C). These high-speed indentations were performed until reaching a pre-set force of 1 nN. Cell elasticity was calculated from the obtained force-displacement curves by applying a Hertzian model, approximating that the sample is isotropic and linearly elastic. Young's (elastic) modulus could be extracted by fitting all force-displacement curves with the following Hertzian model approximation:

$$F = \frac{2E \cdot \tan\alpha}{\pi(1-\nu^2)} \delta^2 \tag{1}$$

where F is the applied force, E is the elastic modulus, ν is the Poisson's ratio (0.5 for a non-compressible biological sample), α is the opening angle of the cone of the cantilever tip, and δ is the indentation depth of the sample. Using the results of the Hertzian model approximation, we identified the Z contact points (specimen surface) and the elastic modulus of the specimens at each pixel, and produced a surface topography map and elastic modulus map of the specimens to estimate cell height and mechanical tension of actin fibers.

RNA-seq analysis. RNA was extracted from CTRL (n=3) and *Thbs1*KO (n=3) cells in static and stretch condition. Total RNA was isolated using TRIZOL reagent (Thermo Fisher) and quality of RNA was examined using an RNA 6000 Pico kit (Agilent) as previously described[9]. An amount of 500 ng total RNA was used for RNA-seq library preparation with NEB NEBNext Poly(A) mRNA Magnetic Isolation Module and ENBNext Ultra Directional RNA Library Prep Kit (New England Biolabs). Two × 36 base paired-end sequencing was performed with NextSeq500 (Illumina) by Tsukuba i-Laboratory LLP (Tsukuba, Japan). FASTQ files were analyzed using CLC Genomics Workbench (Version 10.1.1; Qiagen). Sequences were mapped to rat genome and quantified annotated genes. Transcript expression values were estimated as "reads per kilobase per million reads", and analyzed using Emperical Analysis of DGE tool (Qiagen).

Bioinfomatics analysis. Functional network analyses of genes/proteins with statistically significant expression changes were performed using Ingenuity Pathway Analysis (Ingenuity Systems). Gene Ontology and Reactome pathway analyses were performed using GO Consortium (http://www.geneontology.org). Venn diagram was generated using Venny tool (http://bioinfogp.cnb.csic.es/tools/venny/) from BioinfoGP to identify the transcripts uniquely expressed in each condition.

Mice. C57BL/6J (wild-type) mice were purchased from Charles River, Japan and *Thbs1* null mice were purchased from Jackson Laboratory (B6.129S2-*Thbs1^tm1Hyn*/J) and crossed with C57BL/6 mice for line maintenance. Male mice were used for experiments to exclude hormonal regulation by estrogen. All mice were kept on a 12 h/12 h light/dark cycle under specific pathogen free condition and all animal protocols were approved by the Institutional Animal Experiment Committee of the University of Tsukuba.

Transverse aortic constriction (TAC). Eight-week-old male *Thbs1KO* mice or control littermates underwent TAC using a standard surgical protocol[10]. Briefly, anesthetized mice were placed in a spine position, and aortic constriction was achieved by tying a 6-0 silk suture (Natsume Seisakusho Co., Ltd.) against a 25-gauge blunt needle (TERUMO). For the sham group, the same operation was performed without ligating the aorta. Mice were kept for 5 weeks after TAC and the aortas were harvested.

Carotid artery ligation. Eight-week-old male C57BL/6 or *Thbs1*KO mice were used for carotid artery ligation as previously described[11]. Briefly, the left common carotid artery was dissected free of connective tissues and permanently ligated proximally to the bifurcation. At 1, 2, or 3 weeks after surgery, mice were euthanized, perfused, and right and left carotid arteries were harvested and embedded in optimal cutting temperature compound. Serial cross sections were prepared from the ligature toward the aortic arch with 10 μm intervals until neointima disappeared.

Production of lentivirus encoding siRNA and infection. Lentivirus expressing GFP (LV011-a) and siRNA targeting mouse *Thbs1* was purchased from Applied Biological Materials (abm) Inc. *Thbs1*-set siRNA (i043193) sequences were as follows, #si-RNA463 (AGCATCACGCTGTTTGTTCAAGAGGACCG); #siRNA1586 (GCAAAGACTGTGTTGG-CGATGTGACAGAA); #si-RNA2756 (AGAAGGACTCTGATGGTGATGGCCGAGGT); #siRNA3106 (TT-CTACGTTGTGATGTGGAAACAAGTCAC). siRNA lentivector and 3rd Generation Packaging System mix (LV053, abm Inc.) were co-transfected into 293T cells. Supernatant containing the lentiviral particles was collected 48 h after transfection and concentration of lentivirus was conducted using Lenti-X™ Concentrator. Transfection efficiency was calculated by using GFP-positive cells. For in vivo infection, the virus solution (100 μl, 1×10^7 IU/ml) was inoculated into the tail vein 2 weeks after carotid artery ligation.

Immunohistochemistry, Histology and morphometric analysis. Aortas were harvested and fixed with 4% paraformaldehyde and embedded in paraffin. Five-micrometer sections were stained with H&E for routine histology and Hart's staining for detection of elastic fibers. For immunohistochemistry, primary antibody is shown in Online Table I. Incubation was performed overnight at 4 °C. After washing, anti-rabbit HRP-conjugated second antibody (1:1000, Bio-rad) was added for 1h. TaKaRa DAB Substrate (Takara) was used for detection and hematoxylin was used for counterstaining. Images were digitally captured with Axio Imager Z2 (ZEISS). Morphometric analysis was performed with NIH ImageJ software as previously described[4].

Statistical analysis. All experiments are presented as means ± standard error of the mean (SEM). Statistical analysis was performed using Prism 7 (Graph Pad). *P* < 0.05 denotes statistical significance.

Data availability. The acquisition of online accession numbers for the secretome data is jPOST ID : JPST000600/PXD013915 (http://jpostdb.org) and for the RNA-seq data is GSE131750 (GEO accession). All data supporting the findings of this study are available from the corresponding authors on reasonable request.

References

1. Fukumoto M, Ijuin T, Takenawa T. Pi(3,4)p2 plays critical roles in the regulation of focal adhesion dynamics of mda-mb-231 breast cancer cells. *Cancer Sci*. 2017;108:941-951

2. Uechi Y, Bayarjargal M, Umikawa M, Oshiro M, Takei K, Yamashiro Y, Asato T, Endo S, Misaki R, Taguchi T, Kariya K. Rap2 function requires palmitoylation and recycling endosome localization. *Biochem Biophys Res Commun*. 2009;378:732-737

3. Kaji N, Ohashi K, Shuin M, Niwa R, Uemura T, Mizuno K. Cell cycle-associated changes in slingshot phosphatase activity and roles in cytokinesis in animal cells. *J Biol Chem*. 2003;278:33450-33455

4.   Yamashiro Y, Thang BQ, Shin SJ, Lino CA, Nakamura T, Kim J, Sugiyama K, Tokunaga C, Sakamoto H, Osaka M, Davis EC, Wagenseil JE, Hiramatsu Y, Yanagisawa H. Role of thrombospondin-1 in mechanotransduction and development of thoracic aortic aneurysm in mouse and humans. *Circ Res*. 2018;123:660-672

5.   Monteiro AC, Luissint AC, Sumagin R, Lai C, Vielmuth F, Wolf MF, Laur O, Reiss K, Spindler V, Stehle T, Dermody TS, Nusrat A, Parkos CA. Trans-dimerization of jam-a regulates rap2 and is mediated by a domain that is distinct from the cis-dimerization interface. *Mol Biol Cell*. 2014;25:1574-1585

6.   Gera N, Swanson KD, Jin T. Beta-arrestin 1-dependent regulation of rap2 is required for fmlp-stimulated chemotaxis in neutrophil-like hl-60 cells. *J Leukoc Biol*. 2017;101:239-251

7.   Masuda T, Tomita M, Ishihama Y. Phase transfer surfactant-aided trypsin digestion for membrane proteome analysis. *J Proteome Res*. 2008;7:731-740

8.   Nagayama K, Uchida K, Sato A. A novel micro-grooved collagen substrate for inducing vascular smooth muscle differentiation through cell tissue arrangement and nucleus remodeling. *J Mech Behav Biomed Mater*. 2019;90:295-305

9.   Morito N, Yoh K, Usui T, Oishi H, Ojima M, Fujita A, Koshida R, Shawki HH, Hamada M, Muratani M, Yamagata K, Takahashi S. Transcription factor mafb may play an important role in secondary hyperparathyroidism. *Kidney Int*. 2018;93:54-68

10.   Yamashiro Y, Papke CL, Kim J, Ringuette LJ, Zhang QJ, Liu ZP, Mirzaei H, Wagenseil JE, Davis EC, Yanagisawa H. Abnormal mechanosensing and cofilin activation promote the progression of ascending aortic aneurysms in mice. *Sci Signal*. 2015;8:ra105

11.   Spencer JA, Hacker SL, Davis EC, Mecham RP, Knutsen RH, Li DY, Gerard RD, Richardson JA, Olson EN, Yanagisawa H. Altered vascular remodeling in fibulin-5-deficient mice reveals a role of fibulin-5 in smooth muscle cell proliferation and migration. *Proc Natl Acad Sci U S A*. 2005;102:2946-2951

Online Figures and Figure legends

A

B

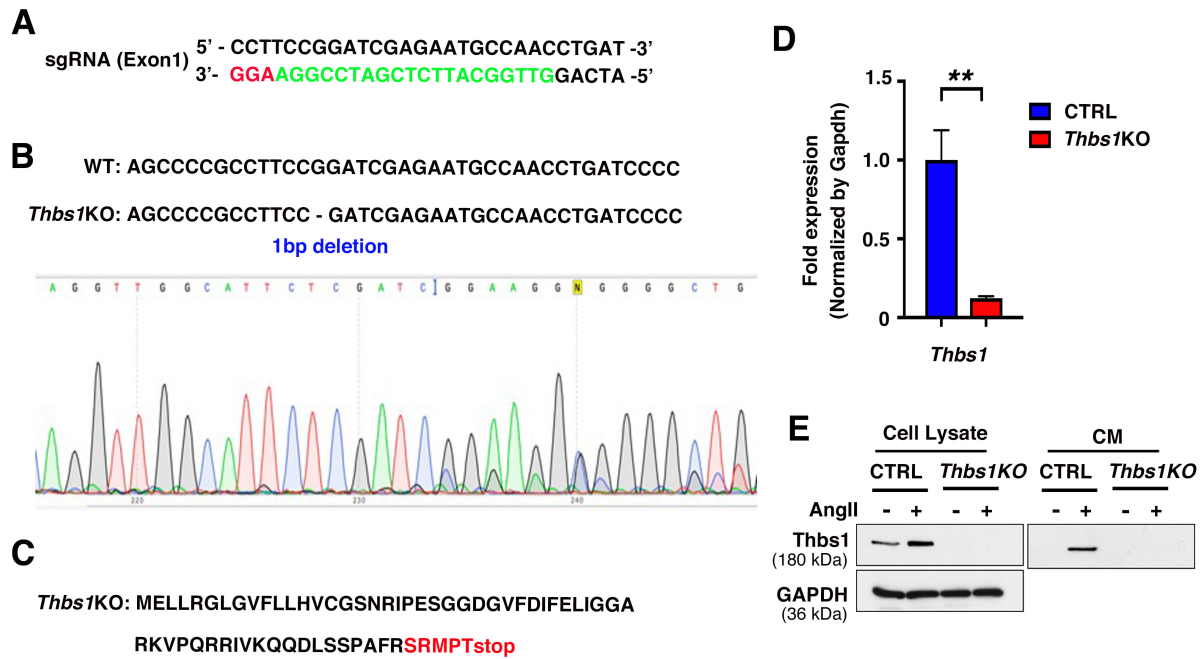|	Proteins	Peptides
Static	656	5344
Stretch	735	6831
Stretch+BFA	685	4912
All	870	8493
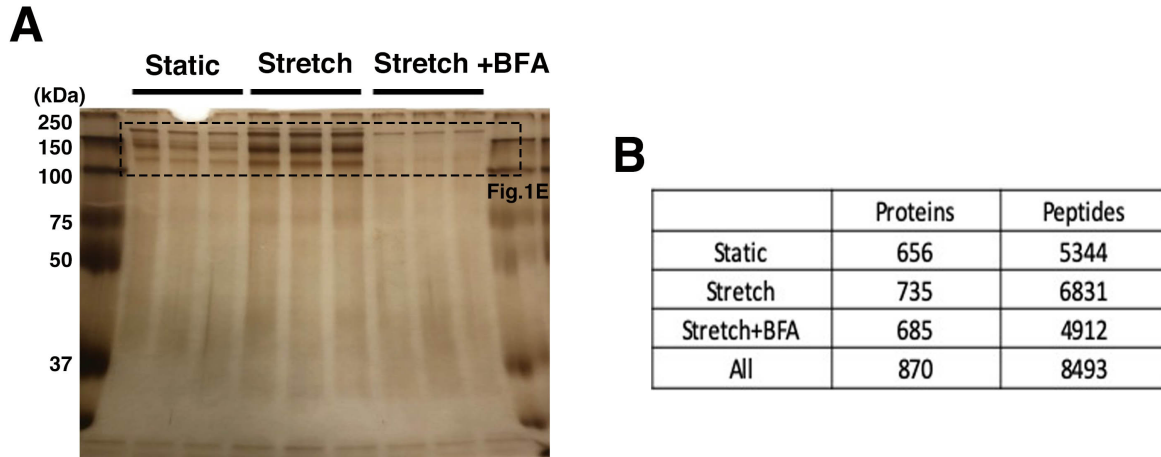
Online Figure I. Secretome analysis of rat vascular SMCs under cyclic stretch. A, Entire image of silver staining of conditioned media provided in Fig.1E. **B,** Table of identified proteins under static or stretch condition.

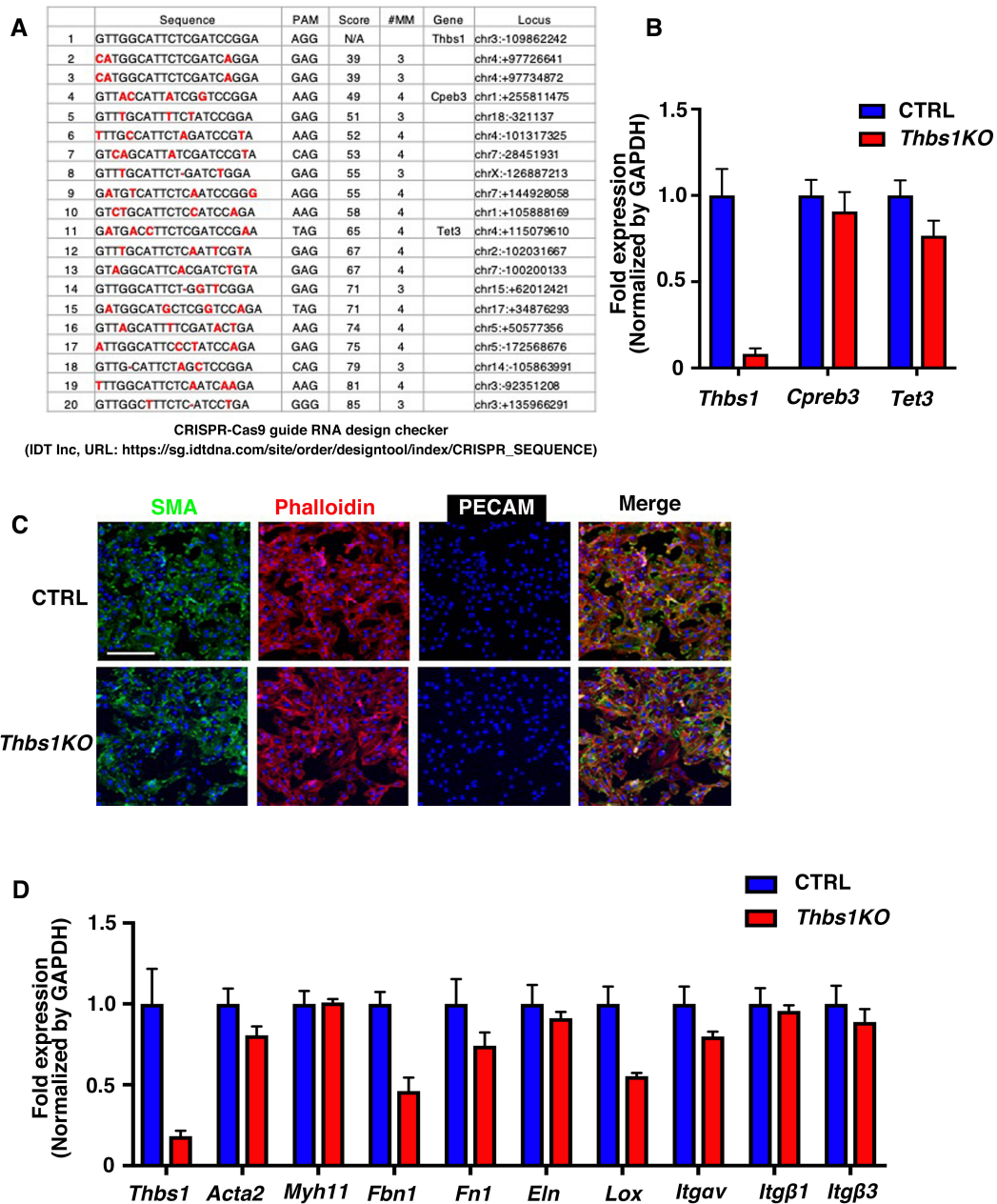| No	Symbol	Name	Num. of Peptide	Ratio			T-Test		
				Stretch/Static	Stretch/Stretch+BFA	Stretch+BFA/Static	Stretch/Static	Stretch/Stretch+BFA	Stretch+BFA/Static
1	Lum	Lumican	13	7.64	21.42	0.36	2.09E-05	2.84E-04	5.06E-05
2	Thbs1	Thrombospondin 1	42	5.80	13.40	0.43	6.23E-06	1.00E-04	1.84E-04
3	Col11a1	Collagen alpha-1(XI) chain	15	4.88	6.53	0.75	1.59E-05	1.17E-04	6.49E-02
4	Col3A1	Collagen alpha-1(III) chain	211	4.85	15.08	0.32	8.83E-06	6.83E-05	9.59E-04
5	Postn	Periostin	17	4.75	6.89	0.69	2.60E-04	1.93E-03	2.53E-03
6	EPYC	Epiphycan	18	4.70	20.24	0.23	1.70E-05	1.86E-04	1.46E-06
7	Fbn1	Fibrillin 1	108	4.67	10.21	0.46	5.65E-06	7.29E-05	2.97E-04
8	Mmp2	Matrix Metalloproteinase-2	42	4.65	16.28	0.29	1.18E-04	8.20E-04	2.16E-06
9	Bgn	Biglycan	44	4.61	36.24	0.13	1.57E-04	6.72E-04	1.50E-03
10	Col6a2	Collagen type VI alpha 2 chain	12	4.54	6.20	0.73	4.48E-03	1.69E-02	1.56E-02
11	Col4a2	Collagen type IV alpha 2 chain	22	4.46	9.77	0.46	1.39E-04	1.02E-03	3.39E-06
12	Ogn	Osteoglycin	8	4.43	8.18	0.54	2.69E-04	1.60E-03	3.89E-03
13	Nid2	Nidogen-2	34	4.39	6.39	0.69	1.96E-04	1.22E-03	4.56E-02
14	Col5a1	Collagen alpha-1(V) chain	29	4.28	7.35	0.58	2.18E-05	2.23E-04	2.53E-03
15	Serpinf2	Alpha-2 antiplasmin	18	4.27	14.51	0.29	9.79E-03	2.17E-02	1.87E-03
16	Ltbp2	Latent-transforming growth factor beta-binding protein 2	21	4.19	6.11	0.69	5.12E-06	9.69E-05	3.42E-05
17	Timp1	Metalloproteinase inhibitor 1	16	4.19	12.93	0.32	1.87E-05	1.16E-04	7.80E-04
18	Fn1	Fibronectin	300	4.17	7.19	0.58	1.10E-04	8.98E-04	2.04E-03
19	Vcan	Versican core protein (Fragments)	10	4.11	4.80	0.86	3.14E-04	2.05E-03	2.23E-01
20	Igfbp7	Insulin-like growth factor binding protein 7, isoform CRA_b	26	4.05	28.38	0.14	1.20E-04	5.67E-04	2.48E-04
21	B2m	Beta-2-microglobulin	5	3.97	6.62	0.60	5.97E-05	5.55E-04	7.83E-04
22	Lox	Lysyl Oxidase	4	3.93	5.25	0.75	5.52E-04	4.71E-04	3.74E-01
23	Sparc	Secreted protein acidic and cysteine rich	58	3.92	32.51	0.12	1.03E-04	5.40E-04	2.64E-05
24	Cxcl1	Growth-regulated alpha protein	5	3.90	16.64	0.23	8.53E-05	2.85E-04	2.27E-03
25	C1r	Complement C1r	37	3.84	17.04	0.23	5.62E-05	3.70E-04	1.47E-05
26	Col1a2	Collagen alpha-2(I) chain	438	3.84	17.30	0.22	5.28E-08	3.98E-07	4.45E-06
27	Hspg2	Heparan Sulfate proteoglycan 2	67	3.80	6.15	0.62	3.53E-03	1.17E-02	1.31E-02
28	Col4a1	Collagen type IV alpha 1 chain	8	3.79	17.94	0.21	1.37E-05	1.24E-04	4.27E-06
29	Sod1	Superoxide dismutase 1	18	3.73	22.80	0.16	2.42E-04	9.24E-04	3.54E-04
30	Timp2	Metalloproteinase inhibitor 2	17	3.71	16.34	0.23	3.83E-05	2.76E-04	2.82E-06
31	Fstl1	Follistatin-related protein 1	34	3.70	30.34	0.12	2.65E-04	1.10E-03	3.14E-06
32	Col1a1	Collagen alpha-1(I) chain	586	3.67	10.71	0.34	8.08E-06	6.12E-05	2.44E-04
33	Cdh13	Cadherin 13	3	3.66	3.81	0.96	6.36E-05	8.08E-04	1.76E-01
34	C1s	Complement C1s subcomponent	9	3.57	15.26	0.23	2.97E-05	2.16E-04	1.89E-05
35	Igfbp6	Insulin-like growth factor-binding protein 6	7	3.56	13.33	0.27	2.33E-04	3.81E-04	7.42E-03
36	Fbln2	Fibulin 2	43	3.54	4.16	0.85	3.61E-06	1.22E-04	1.54E-01
37	Ecm1	Extracellular matrix protein 1	12	3.54	12.17	0.29	7.76E-06	3.12E-05	3.04E-04
38	Col6a1	Collagen type VI alpha 1 chain	12	3.53	5.49	0.64	2.16E-04	1.44E-03	2.31E-04
39	Tcn2	Transcobalamin-2	12	3.51	10.61	0.33	3.29E-04	1.47E-03	1.52E-05
40	Il1rl1	Interleukin-1 receptor-like 1	3	3.50	4.10	0.85	4.58E-04	2.77E-03	1.33E-01
41	Rnase4	Ribonuclease 4	3	3.45	10.26	0.34	4.78E-05	3.14E-04	4.12E-05
42	Spp1	Osteopontin	22	3.40	15.29	0.22	5.10E-03	1.07E-02	7.08E-06
43	Inhba	Inhibin beta A chain	6	3.36	5.91	0.57	1.29E-04	6.44E-04	4.20E-03
44	Loxl3	Lysyl oxidase-like 3	7	3.35	5.04	0.67	1.36E-06	1.99E-05	2.62E-04
45	Eln	Elastin	13	3.35	3.35	1.00	6.17E-04	4.80E-03	#DIV/0!
46	Lamb1	Laminin subunit beta 1	14	3.28	3.57	0.92	2.23E-03	1.10E-02	1.63E-01
47	Nucb1	Nucleobindin-1	27	3.27	10.99	0.30	7.79E-06	7.26E-05	7.89E-06
48	Plod2	Procollagen-lysine,2-oxoglutarate 5-dioxygenase 2	5	3.25	3.79	0.86	6.74E-03	2.29E-02	5.06E-01
49	Pcolce	Procollagen C-endopeptidase enhancer 1	37	3.24	17.52	0.19	5.76E-05	3.02E-04	7.95E-06
50	Clstn1	Calsyntenin-1	24	3.21	9.28	0.35	1.68E-05	9.09E-05	1.80E-04
51	Col5a2	Collagen type V alpha 2 chain	69	3.19	8.69	0.37	2.94E-05	2.31E-04	2.05E-06
52	Ccl2	C-C motif chemokine 2	5	3.18	14.82	0.21	4.42E-04	1.10E-03	1.01E-03
53	Svep1	Sushi, von Willebrand factor type A, EGF and pentraxin domain-containing protein 1	14	3.17	3.96	0.80	3.34E-05	3.75E-04	2.22E-03
54	Srpx2	Sushi repeat-containing protein SRPX2	4	3.15	4.81	0.65	1.09E-05	1.35E-04	8.35E-05
55	Pin1	Peptidylprolyl isomerase	8	3.11	5.42	0.57	1.42E-04	5.34E-04	1.32E-02
56	Clu	Clusterin	24	3.11	18.06	0.17	9.96E-05	3.74E-04	6.98E-05
57	Lamc1	Laminin subunit gamma 1	24	3.09	3.83	0.81	2.01E-03	8.77E-03	1.11E-02
58	Pxdn	Peroxidasin	3	3.09	3.99	0.77	3.19E-03	1.16E-02	2.80E-02
59	Nid1	Nidogen-1 (Fragment)	8	3.06	8.55	0.36	1.59E-04	7.57E-04	9.59E-06
60	Atp5b	ATP synthase subunit beta, mitochondrial	3	3.04	3.44	0.88	8.36E-04	3.97E-03	3.91E-01
61	Lgals3bp	Galectin-3-binding protein	21	2.99	11.79	0.25	5.39E-04	7.44E-04	4.46E-03
62	Htra1	Serine protease HTRA1	20	2.94	5.32	0.55	2.96E-04	1.47E-03	4.64E-04
63	Ltbp1	Latent-transforming growth factor beta-binding protein 1	8	2.93	3.32	0.88	2.96E-04	1.91E-03	1.18E-01
64	Acan	Aggrecan core protein	7	2.93	2.94	1.00	1.24E-03	8.02E-03	3.74E-01
65	Olfml3	Olfactomedin-like protein 3	6	2.92	2.73	1.07	1.45E-03	1.84E-03	8.41E-01
66	Cpe	Carboxypeptidase E	7	2.91	5.33	0.55	8.69E-04	3.19E-03	3.12E-04
67	Oaf	Out at first protein homolog	3	2.91	3.21	0.91	1.90E-04	1.58E-03	6.06E-02
68	Col8a1	Collagen type VIII alpha 1 chain	11	2.90	2.82	1.03	1.10E-03	8.17E-03	6.39E-01
69	Nov	Protein NOV homolog	4	2.77	6.47	0.43	4.14E-04	1.38E-03	2.66E-04
70	Col18a1	Collagen type XVIII alpha 1 chain	17	2.75	7.72	0.36	3.29E-04	1.11E-03	6.31E-05
71	Cst3	Cystatin-C	9	2.70	10.90	0.25	9.19E-04	8.24E-05	1.48E-02
72	Fbln5	Fibulin-5	9	2.69	6.68	0.40	4.91E-04	1.67E-03	9.44E-07
73	Syncrip	Heterogeneous nuclear ribonucleoprotein Q	3	2.67	2.42	1.10	6.05E-03	6.63E-06	8.51E-01
74	Ctsb	Cathepsin B	41	2.63	5.35	0.49	6.15E-05	6.22E-05	2.88E-04
75	Minpp1	Multiple inositol polyphosphate phosphatase 1	3	2.53	2.68	0.95	4.47E-03	1.89E-02	1.54E-02
76	Csf1	Macrophage colony-stimulating factor 1	9	2.53	7.14	0.35	4.08E-04	1.13E-03	6.14E-05
77	Ctsl	Cathepsin L1	10	2.50	5.81	0.43	3.54E-05	3.64E-05	8.06E-04
78	Efemp1	EGF-containing fibulin extracellular matrix protein 2	8	2.47	4.63	0.53	1.67E-03	3.76E-03	2.84E-03
79	C3	Complement C3	20	2.27	3.47	0.65	3.84E-05	4.87E-05	3.00E-03
80	Pai1	Plasminogen activator inhibitor 1	16	2.27	6.86	0.33	5.37E-03	6.78E-03	3.70E-04
81	Npc2	NPC intracellular cholesterol transporter 2	8	2.24	2.41	0.93	2.15E-04	1.53E-03	1.30E-01
82	Ctgf	Connective tissue growth factor	13	2.19	6.79	0.32	7.35E-04	1.07E-03	3.50E-04
83	Pdgfrl	Platelet-derived growth factor receptor-like protein	3	2.12	2.21	0.96	1.45E-05	1.65E-05	3.74E-01
84	Rps8	40S ribosomal protein S8	6	0.48	0.42	1.14	6.40E-04	3.59E-05	1.39E-01
85	Rps16	40S ribosomal protein S16	5	0.35	0.29	1.21	4.91E-03	3.72E-02	4.24E-01
86	Rps26	40S ribosomal protein S26	3	0.41	0.78	0.53	9.30E-04	8.81E-01	2.56E-02
87	Rpl30	60S ribosomal protein L30	4	0.41	0.38	1.07	1.56E-03	8.52E-03	5.85E-01

Online Figure II. List of identified secreted proteins from rat vascular SMCs under cyclic stretch.
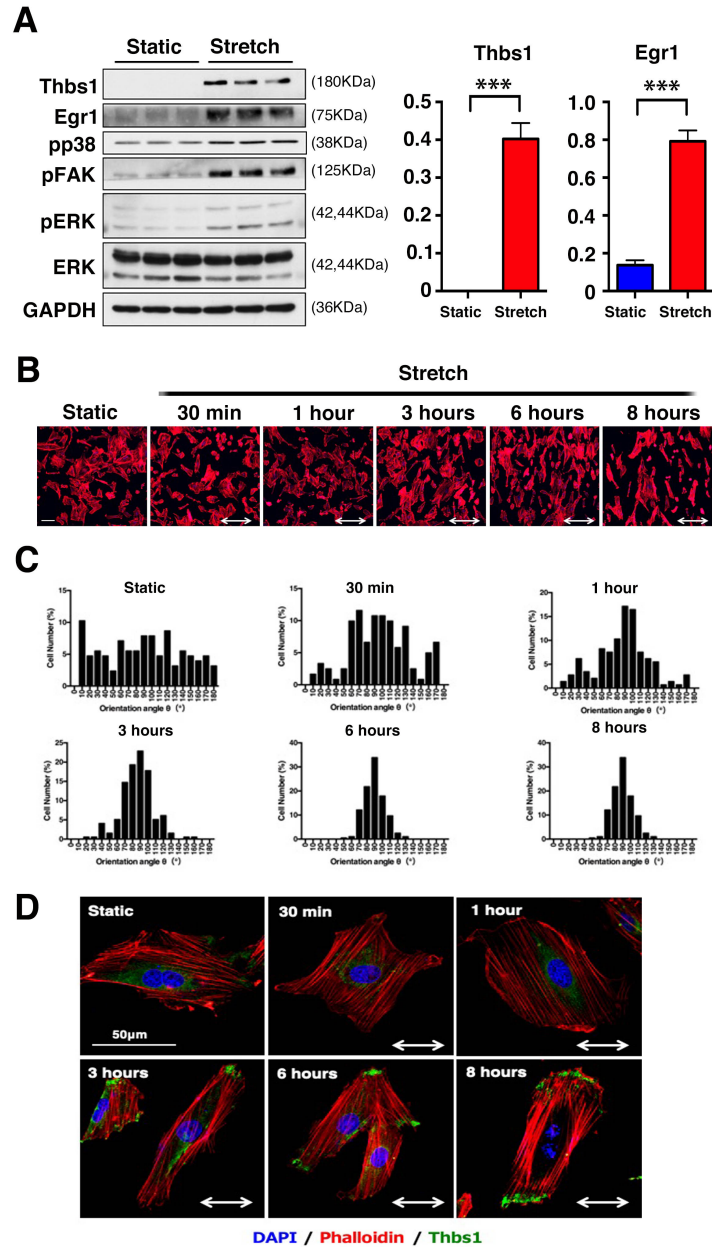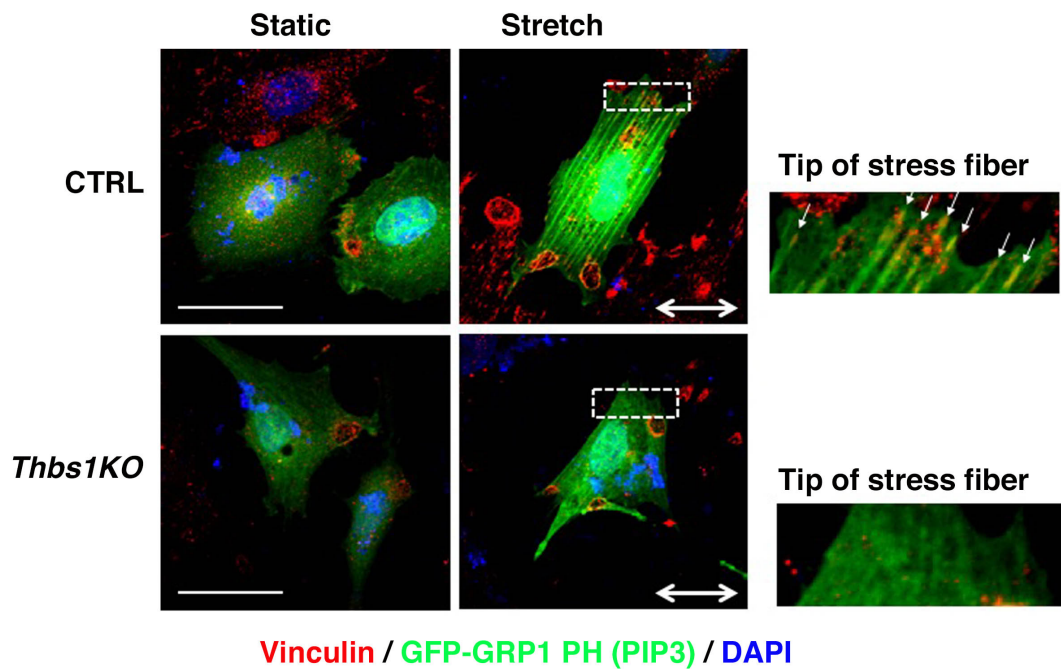
Online Figure III. Thbs1 expression during cyclic stretch. Rat vascular SMCs were subjected to cyclic stretch (1.0 Hz, 20% strain, 8h). **A,** Cell lysates were analyzed using Western blotting with indicated antibodies (n=3). Quantification graphs are shown on the right. Bars are means ± SEM. ***$P<0.001$, unpaired t-test. **B-C,** Immunostaining with Phalloidin (red). Cell orientation was analyzed by measuring the orientation angle (θ) of the long axis of the ellipse relative to the stretch axis. 50-100 cells were evaluated in each condition (n=3). Bars are 50 μm. Two-way arrows indicates stretch direction. **D,** Representative immunostaining of SMCs at an indicated time after stretch. Phalloidin (red), Thbs1 (green), and DAPI (blue). n=3.
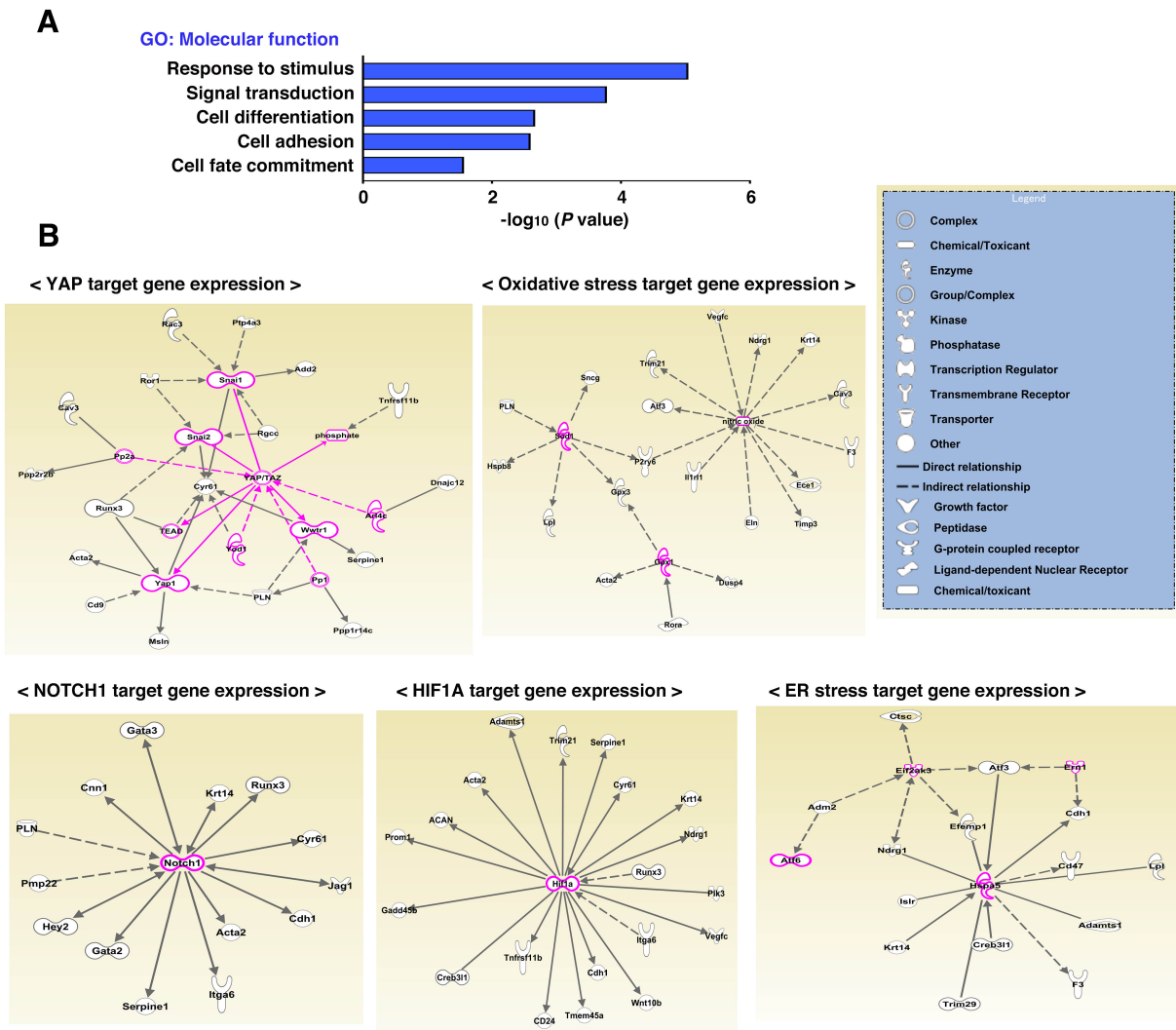
A

sgRNA (Exon1)   5' - CCTTCCGGATCGAGAATGCCAACCTGAT -3'
                 3'- GGAAGGCCTAGCTCTTACGGTTGGACTA -5'

B

WT: AGCCCCGCCTTCCGGATCGAGAATGCCAACCTGATCCCC

Thbs1KO: AGCCCCGCCTTCC - GATCGAGAATGCCAACCTGATCCCC

1bp deletion

A G G T T G G C A T T C T C G A T C] G G A A G G N G G G G C T G

C

Thbs1KO: MELLRGLGVFLLHVCGSNRIPESGGDGVFDIFELIGGA

RKVPQRRIVKQQDLSSPAFRSRMPTstop

D

E

Online Figure IV. *Thbs1* **deletion by CRISPR-Cas9 in rat vascular SMCs. A,** sgRNA sequence (green) targeting exon1 of *Thbs1*. PAM (protospacer adjacent motif) sequence is shown in red. **B,** Sequence comparison between *Thbs1*KO cell line (*Thbs1*KO) and control (CTRL) cell line. **C,** Amino acid sequence for *Thbs1*KO. The altered amino acid sequences are shown in red and stop codon appeared in Exon 1 of Thbs1 due to a frame shift (1bp deletion). **D,** qPCR analysis confirming the efficiency of gene deletion in rat vascular SMCs. Bars are means ± SEM. **$**P < 0.01$, unpaired *t*-test. **E,** CTRL and *Thbs1*KO cells cultured in serum-free media for 24 h, then stimulated with Ang II (100 nM) for 6 h. Cell lysates and conditioned medium (CM) were analyzed using Western blotting with indicated antibodies. n=3.

12

A

	Sequence	PAM	Score	#MM	Gene	Locus
1	GTTGGCATTCTCGATCCGGA	AGG	N/A		Thbs1	chr3:-109862242
2	CATGGCATTCTCGATCAGGA	GAG	39	3		chr4:+97726641
3	CATGGCATTCTCGATCAGGA	GAG	39	3		chr4:+97734872
4	GTTACCATTATCGGTCCGGA	AAG	49	4	Cpeb3	chr1:+255811475
5	GTTTGCATTTTCTATCCGGA	GAG	51	3		chr18:-321137
6	TTTGCCATTCTAGATCCGTA	AAG	52	4		chr4:-101317325
7	GTCAGCATTATCGATCCGTA	CAG	53	4		chr7:-28451931
8	GTTTGCATTCT-GATCTGGA	GAG	55	3		chrX:-126887213
9	GATGTCATTCTCAATCCGGG	AGG	55	4		chr7:+144928058
10	GTCTGCATTCTCCATCCAGA	AAG	58	4		chr1:+105888169
11	GATGACCTTCTCGATCCGAA	TAG	65	4	Tet3	chr4:+115079610
12	GTTTGCATTCTCAATTCGTA	GAG	67	4		chr2:-102031667
13	GTAGGCATTCACGATCTGTA	GAG	67	4		chr7:-100200133
14	GTTGGCATTCT-GGTTCGGA	GAG	71	3		chr15:+62012421
15	GATGGCATGCTCGGTCCAGA	TAG	71	4		chr17:+34876293
16	GTTAGCATTTTCGATACTGA	AAG	74	4		chr5:+50577356
17	ATTGGCATTCCCTATCCAGA	GAG	75	4		chr5:-172568676
18	GTTG-CATTCTAGCTCCGGA	CAG	79	3		chr14:-105863991
19	TTTGGCATTCTCAATCAAGA	AAG	81	4		chr3:-92351208
20	GTTGGCTTTCTC-ATCCTGA	GGG	85	3		chr3:+135966291

CRISPR-Cas9 guide RNA design checker
(IDT Inc, URL: https://sg.idtdna.com/site/order/designtool/index/CRISPR_SEQUENCE)

B

C

SMA   Phalloidin   PECAM   Merge

CTRL

Thbs1KO

D

Online Figure V. Off-target effects on *Thbs1 KO* cells. A, Potential off target list of sgRNA for Thbs1. Red indicates miss march (#MM) nucleotides. **B,** qPCR analysis confirming the expression of *Creb3* and *Tet3* in CTRL and *Thbs1KO* rat vascular SMCs. Bars indicate technical triplicate. **C,** Immunostaining of CTRL or *Thbs1KO* cells with smooth muscle actin (SMA, green), Phalloidin (red) and PECAM (white). Bar is 50 μm. **D,** qPCR analysis for the expression of SMC contractile marker (*Acta2* and *Myh11),* matrix compound (*Fbn1*, *Fn1*, *Eln* and *Lox*) and integrins (*Itgαv, Itgβ1* and *Itgβ3*) in CTRL and *Thbs1KO* rat vascular SMCs. Bars indicate technical triplicate.

Static **Stretch**

CTRL

Thbs1KO

Tip of stress fiber

Tip of stress fiber

Vinculin / **GFP-GRP1 PH (PIP3)** / **DAPI**

Online Figure VI.   Deletion of *Thbs1* affects maturation of FA. Representative Immunostaining of control (CTRL) or *Thbs1*KO cells with vinculin (red) in static or stretch condition. GFP-GRP1-PH (green) and DAPI (blue). White arrows show vinculin deposition onto the tip of actin fibers. (n=3). Two-way arrows indicate stretch direction. Bars are 50 μm.

A

GO: Molecular function

Response to stimulus
Signal transduction
Cell differentiation
Cell adhesion
Cell fate commitment

-log$_{10}$ (*P* value)

B

< YAP target gene expression >

< Oxidative stress target gene expression >

< NOTCH1 target gene expression >

< HIF1A target gene expression >

< ER stress target gene expression >

Legend

- Complex
- Chemical/Toxicant
- Enzyme
- Group/Complex
- Kinase
- Phosphatase
- Transcription Regulator
- Transmembrane Receptor
- Transporter
- Other
- Direct relationship
- Indirect relationship
- Growth factor
- Peptidase
- G-protein coupled receptor
- Ligand-dependent Nuclear Receptor
- Chemical/toxicant

Online Figure VII. Bioinformatic analysis for RNA-seq. A, Functional enrichment analysis of 289 genes in Fig. 4C-D. Top enriched GO terms associated with molecular functions (blue) are shown. **B,** Among 289 genes in Fig. 4C-D, network analysis was performed using YAP, oxidative stress-related gene-, NOTCH1, HIF1A, and ER stress-related gene categories via IPA. Diagrams show direct (solid lines) and indirect (dashed lines) interactions among genes.

15
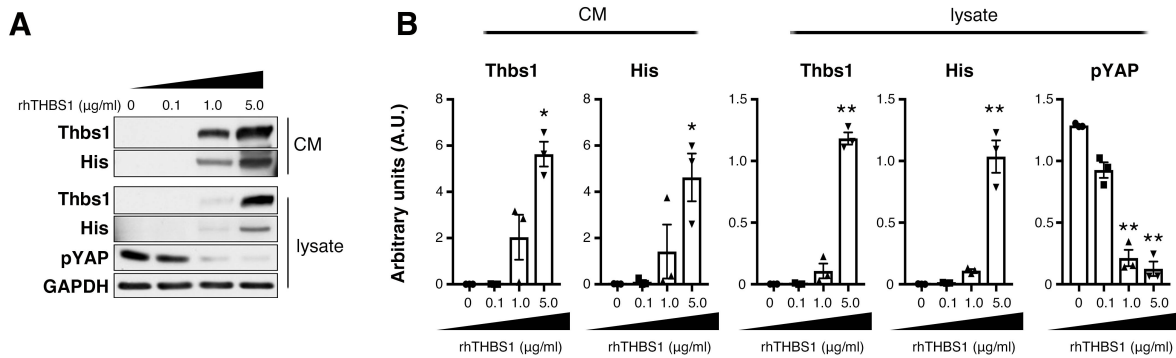
Online Figure VIII. Add-back experiment in *Thbs1KO* cells upon cyclic stretch. A, *Thbs1KO* rat SMCs were treated with or without recombinant human THBS1 with His-tag (rhThbs1;0.1 or 1.0 or 5.0 μg/ml) followed by 24 h of serum starvation and then subjected to uniaxial cyclic stretch (20% strain; 1Hz) for 8h. Representative Western blots shows Thbs1 and His in conditioned medium (CM), Thbs1, His and pYAP levels in cell lysate (n=3). **B,** Quantification graphs shown in right. Bars are means ± SEM. *$P<0.05$, **$P<0.01$, one-way ANOVA.
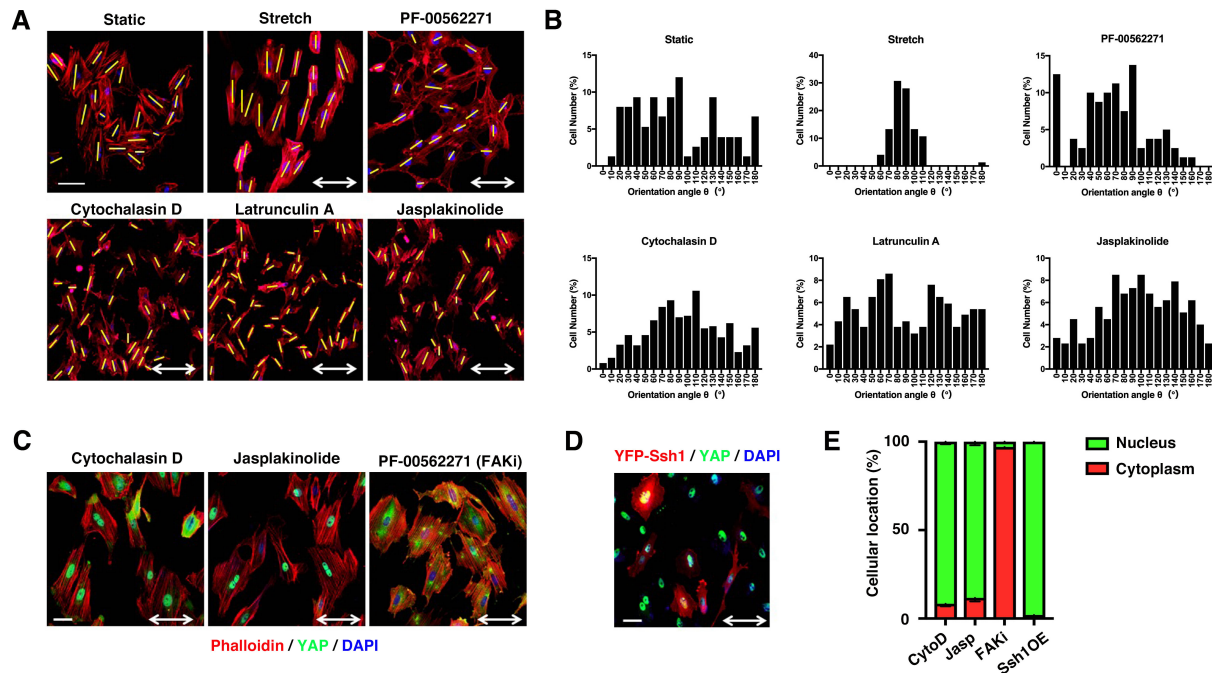
Online Figure IX. FA and actin remodeling are required for proper cell orientation in response to cyclic stretch. Rat vascular SMCs were cultured in serum-free media for 24 h and treated with Cytochalasin D (1 μM), Latrunclin A (1 μM), Jasplakinolide (20 nM) or PF-00562271 (100 nM, FAK inhibitor) and subjected to cyclic stretch (1.0 Hz, 20 % strain, 8h). Bars are 50 μm. Two-way arrows indicate stretch direction. **A,** Immunostaining with Phalloidin (red). **B,** Cell orientation was analyzed by measuring the orientation angle (θ) of the long axis (yellow bars in a) of the ellipse relative to the stretch axis. 50-100 cells were counted in each condition (n=3). **C,** Rat vascular SMCs were cultured in serum-free media for 24 h and treated with Cytochalasin D (1 μM), Jasplakinolide (20 nM), or FAK inhibitor (100 nM) during cyclic stretch (n=3). Representative immunostaining with YAP (green), Phalloidin (red), and DAPI (blue). Two-way arrows indicate stretch direction. Bars are 50 μm. **D,** Rat vascular SMCs were transfected with YFP-Ssh1 (red) and cyclic stretch was performed at 48 h after transfection (n=3). Representative immunostaining with YAP (green) and DAPI (blue). Two-way arrows indicate stretch direction. Bars are 50 μm. **E,** Quantification of YAP localization in C and D. 50-150 cells were evaluated in each experiment (n=3).

A

B
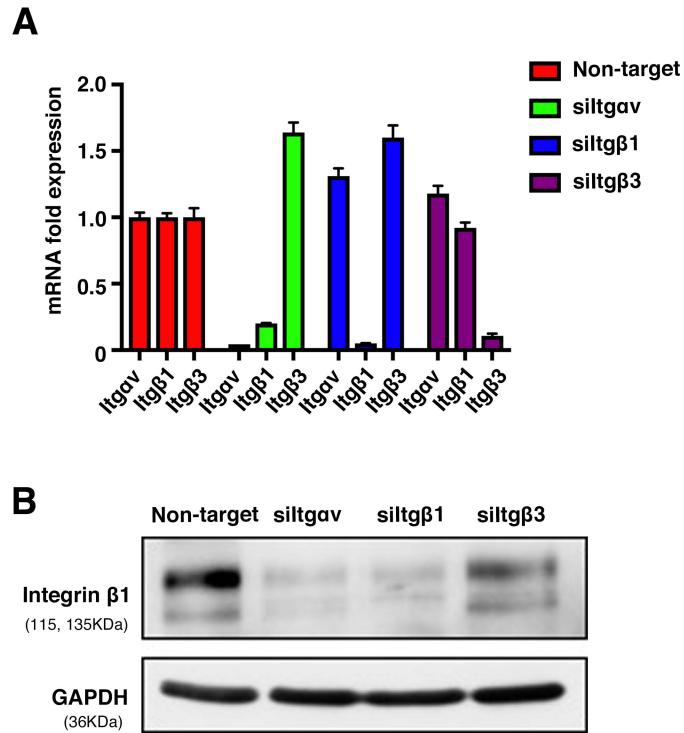
Online Figure X. Deletion of integrins by siRNA. A, Quantitative polymerase chain reaction (qPCR) for confirmation of knockdown of *Itgαv*, *Itgβ1* and *Itgβ3*. Total RNA from small interfering RNA (siRNA)-treated cells was extracted 2 days after transfection. The fold expression relative to scramble siRNA (non-target) is shown. Bars indicate technical triplicate. **B,** Western blot shows integrin β1 levels in siRNA-treated cells.
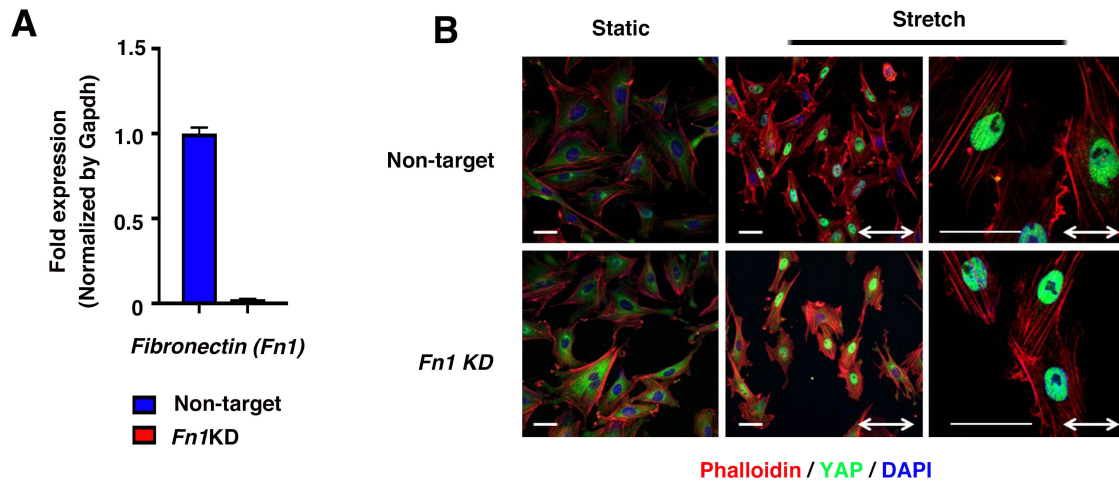
Online Figure XI. Knockdown of fibronectin does not affect stretch-induced nuclear shuttling of YAP. A, qPCR analysis confirming the efficiency of *Fn1* knockdown in rat vascular SMCs. Bars indicate technical triplicate. **B,** Non-target or *Fn1* siRNA-treated rat vascular SMCs were subjected to cyclic stretch (n=3). Immunostaining with YAP (green). Phalloidin (red) and DAPI (blue). Bars are 50 μm.
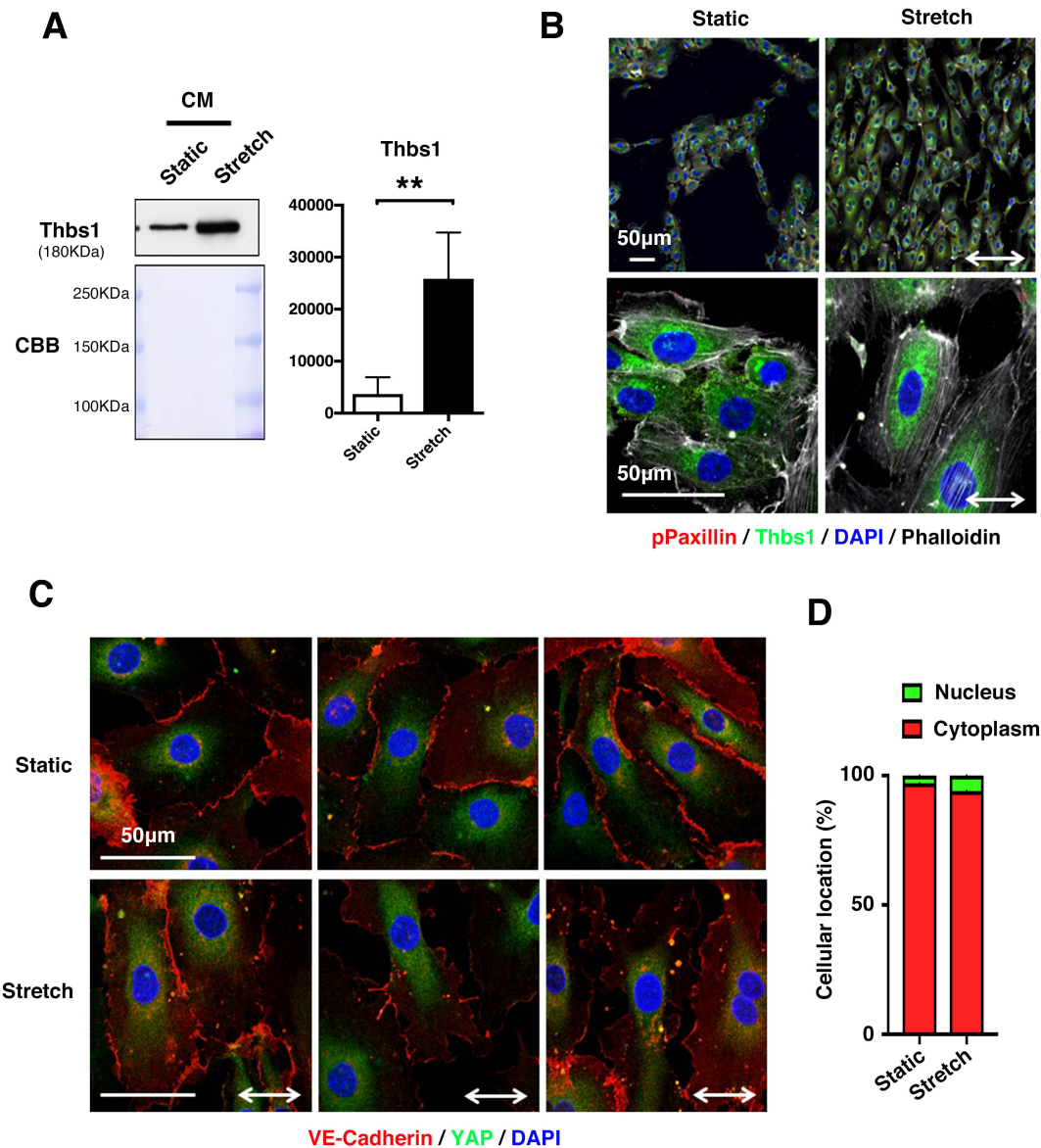
Online Figure XII. Cyclic stretch did not induce translocation of Thbs1 to FAs and nuclear shuttling of YAP in HUVECs. A, Representative Western blot for Thbs1 using the conditioned medium (CM) of HUVEC (n=3) in static or stretch condition. Quantification graph is shown in right. **$P < 0.01$, unpaired t-test. **B,** HUVECs were subjected to cyclic stretch (1.0 Hz, 20% strain, 8 h). Bars are 50 μm. Two-way arrows indicate stretch direction. Immunostaining with p-Paxillin (red), Thbs1 (green), Phalloidin (grey) and DAPI (blue). **C,** Representative immunostaining of HUVEC in static or stretch condition with VE-cadherin (red), YAP (green), and DAPI (blue). **D,** Quantification of YAP localization in 80-100 cells were evaluated in each condition (n=3). YAP localizes in nuclear (green) or cytoplasm (red).
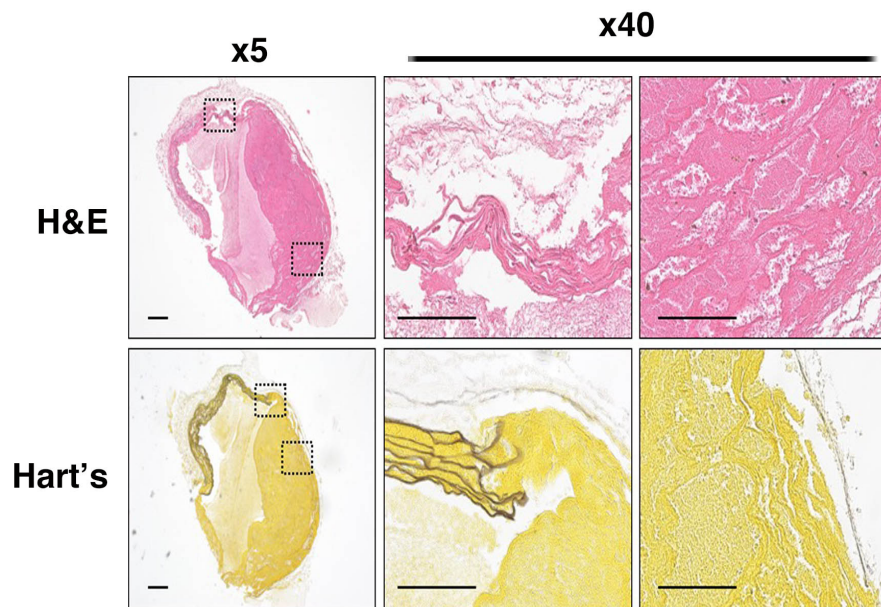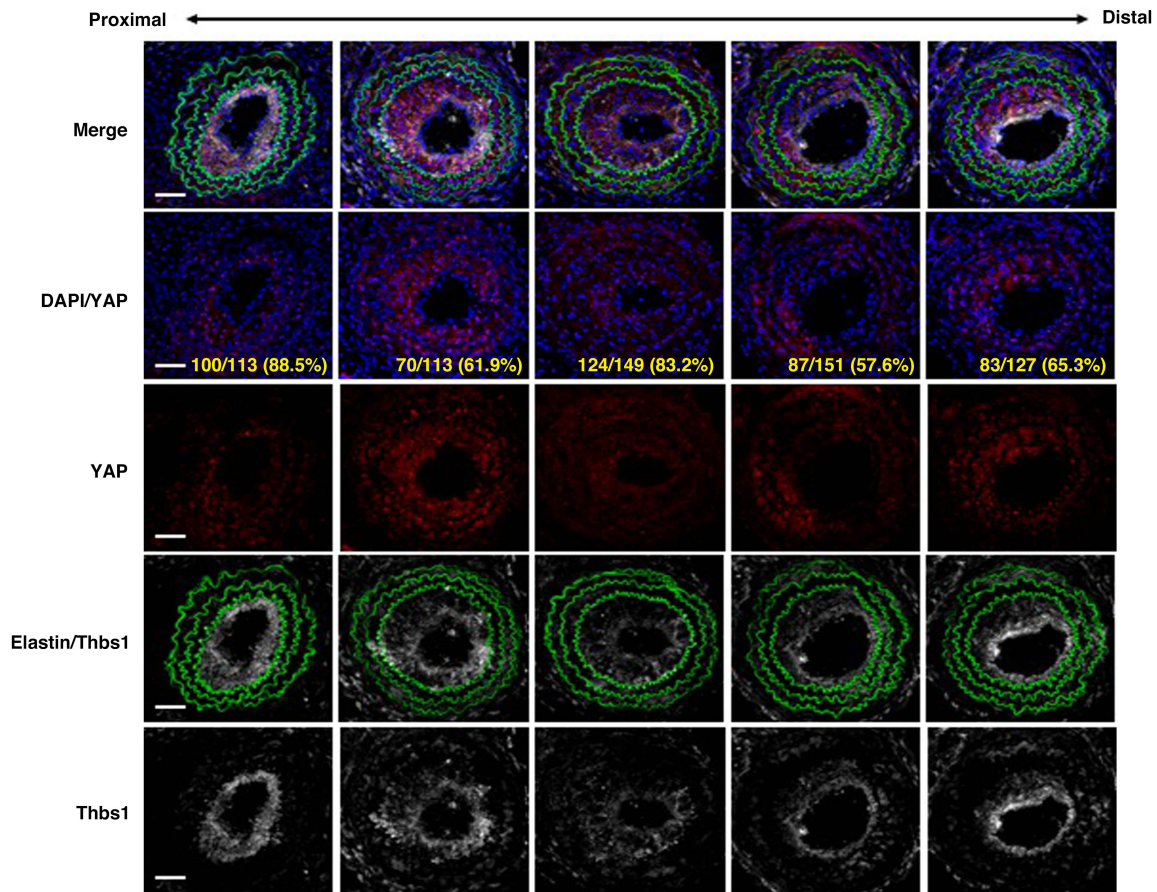
Online Figure XIII. Representative image of *Thbs1* null (*Thbs1KO*) mice with aortic rupture after TAC. H&E and Hart's staining of the ascending aortas in TAC-operated *Thbs1KO* mice. 7 mice died after TAC in *Thbs1KO* mice (Fig. 6B) and 3 of 7 mice showed aortic rupture. Bars are 100 µm.
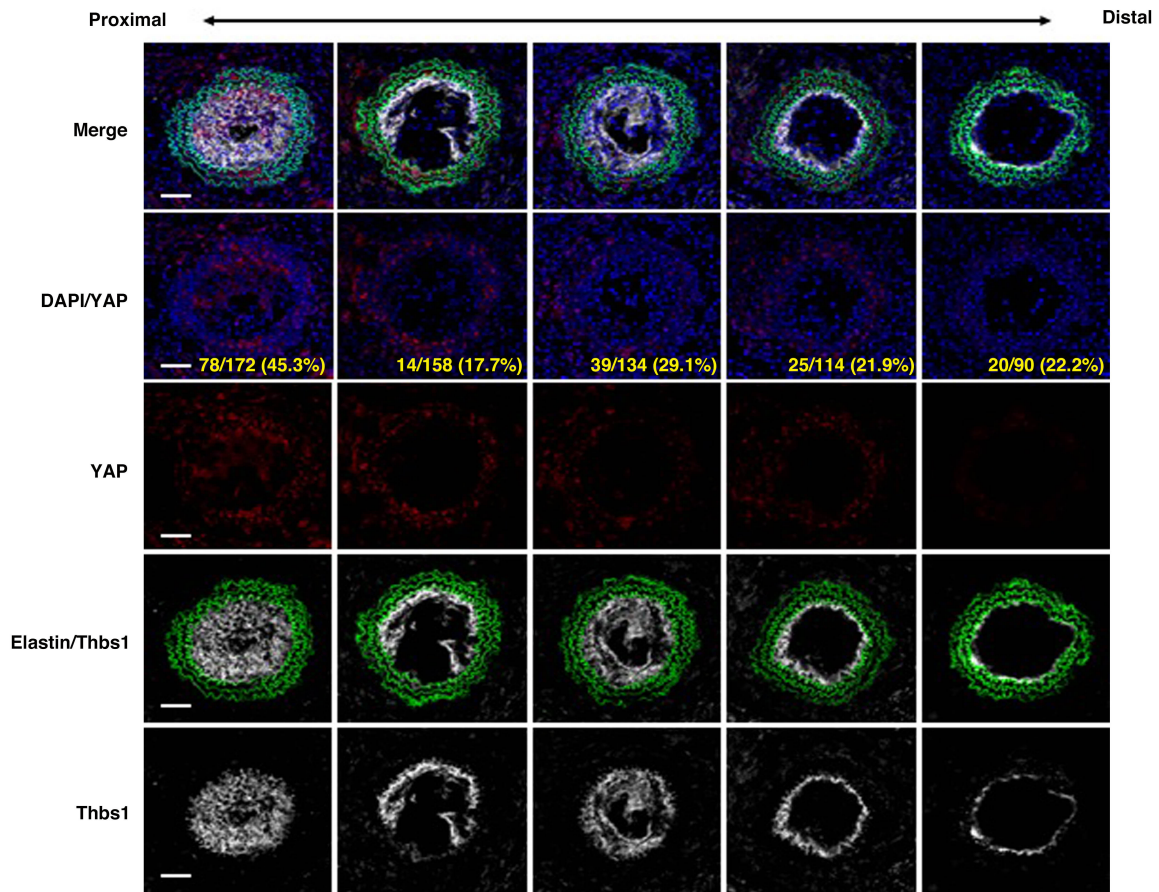
Online Figure XIV. Neointima formation at 1 week after carotid artery ligation. Representative immunostaining of cross sections of ligated arteries with YAP (red) and Thbs1 (white) at 1 week after ligation in WT mice (n=5). DAPI (blue) and auto-fluorescence of elastin (green). Images shows are shown in proximal to distal direction from the ligature point. Bars are 50 μm. Quantification of co-localization with YAP and DAPI using Imaris colocalization software were indicated by yellow (number of nuclear YAP / total number of nucleus).
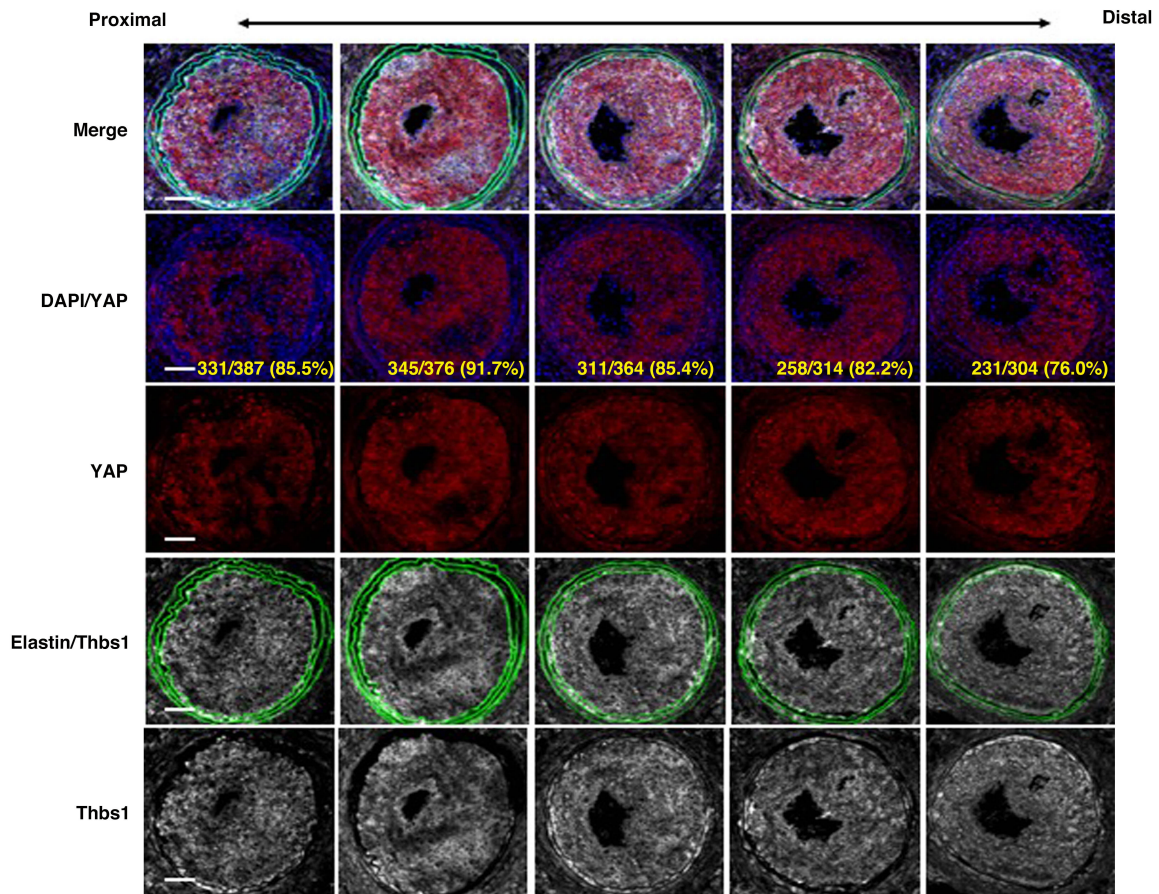
Online Figure XV. Neointima formation at 2 weeks after carotid artery ligation. Representative immunostaining of cross sections of ligated arteries with YAP (red) and Thbs1 (white) at 2 weeks after ligation in WT mice (n=5). DAPI (blue) and auto-fluorescence of elastin (green). Images shows are shown in proximal to distal direction from the ligature point. Bars are 50 μm. Quantification of co-localization with YAP and DAPI using Imaris colocalization software were indicated by yellow (number of nuclear YAP / total number of nucleus).
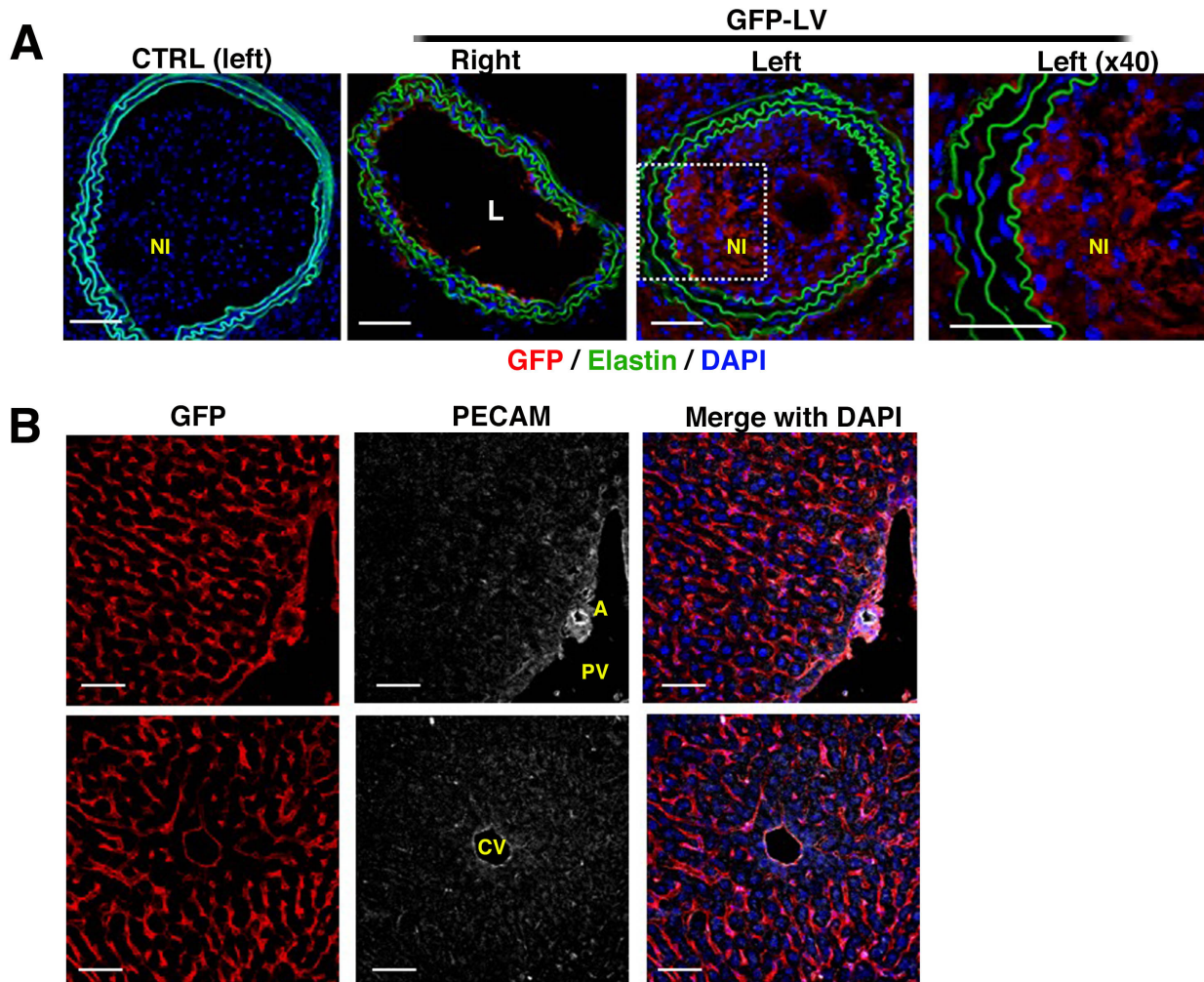
Online Figure XVI. Neointima formation at 3 weeks after carotid artery ligation. Representative immunostaining of cross sections of ligated arteries with YAP (red) and Thbs1 (white) at 3 weeks after ligation in WT mice (n=4). DAPI (blue) and auto-fluorescence of elastin (green). Images shows are shown in proximal to distal direction from the ligature point. Bars are 50 µm. Quantification of co-localization with YAP and DAPI using Imaris colocalization software were indicated by yellow (number of nuclear YAP / total number of nucleus).
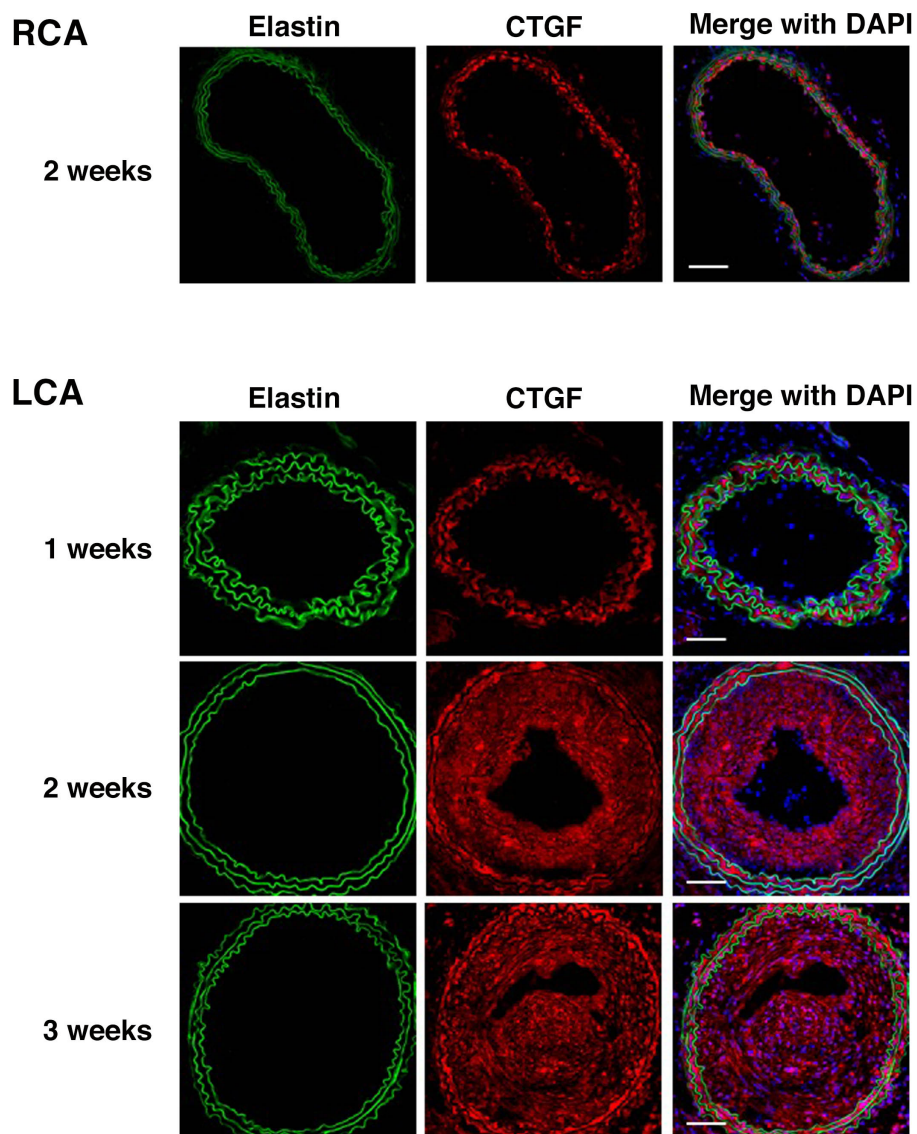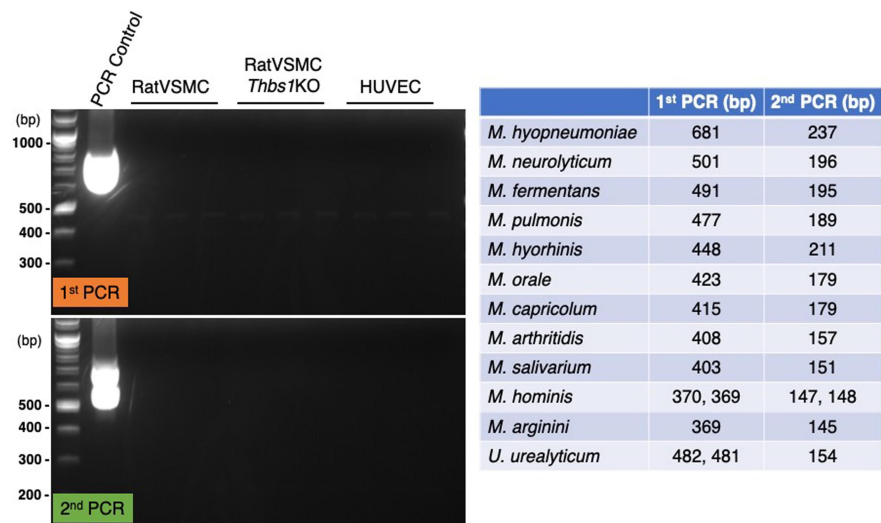
Online Figure XVII. CTGF, downstream target of YAP, is expressed in neointima after 2 weeks of carotid artery ligation. Representative immunostaining of cross sections of right carotid artery (RCA) and left carotid artery (LCA) with CTGF (red) after ligation in WT mice (n=3). DAPI (blue) and auto-fluorescence of elastin (green). Bars are 50 μm.

Online Figure XVIII. Lenti-virus (LV) were delivered from tail vein to neointima of carotid artery. GFP-LV were injected from tail vein 2 weeks after left carotid ligation. **A,** Cross sections of carotid artery at 3 weeks post injury in WT mice (CTRL, n=4), GFP-LV-treated WT mice (n=3). Immunostaining with GFP (red). DAPI (blue) and auto-fluorescence of elastin (green). Note neointima (NI) formation in left carotid artery. Bars are 50 μm. **B,** Liver sections at 3 weeks post injury in GFP-LV-treated WT mice (n=3). Immunostaining with GFP (red), PECAM (white) and DAPI (blue). A: artery, PV: portal vein, CV: central vein. Bars are 50 μm.

	1st PCR (bp)	2nd PCR (bp)
M. hyopneumoniae	681	237
M. neurolyticum	501	196
M. fermentans	491	195
M. pulmonis	477	189
M. hyorhinis	448	211
M. orale	423	179
M. capricolum	415	179
M. arthritidis	408	157
M. salivarium	403	151
M. hominis	370, 369	147, 148
M. arginini	369	145
U. urealyticum	482, 481	154

Online Figure XIX. Cell lines were tested for mycoplasma contamination. 1st PCR and nested 2nd PCR results are shown (n=3). Control template was used as positive control for PCR. The table shows each PCR product size (bp) for *Mycoplasma.*

Online Table I. Antibodies used in this study

Western blot analysis

Antibody	Dilution	Source	Catalog number
Thbs1	1:1000	NeoMarkers	MS-421
GAPDH	1:1000	Cell Signaling	# 2118
pERK1/2	1:500	Cell Signaling	# 4376
ERK	1:1000	Cell Signaling	# 9102
Egr1	1:500	Cell Signaling	# 4154
pp38	1:500	Cell Signaling	#4511
pFAK	1:500	Cell Signaling	#3283
Integrin αv	1:500	Cell Signaling	#4711
Integrin β1	1:500	Cell Signaling	#4706
pYAP	1:500	Cell Signaling	#4911
pLATS1 (T1079)	1:500	Cell Signaling	#8654
His	1:1000	MBL Life Science	D291-3

Immunostaining

Antibody	Dilution	Source	Catalog number
Thbs1	1:200	NeoMarkers	MS-421
Rhodamine Phalloidin	1:500	Cytoskeleton	# PHDR1
pPaxillin (Tyr118)	1:200	Santa Cruz Biotechnology	sc-14036
Integrin αv (N-19)	1:200	Santa Cruz Biotechnology	sc-6616
Integrin β1 (N-20)	1:200	Santa Cruz Biotechnology	sc-6622
Integrin β3 (H-96)	1:200	Santa Cruz Biotechnology	sc-14009
YAP	1:200	Cell Signaling	#14074
Vinculin	1:200	Invitrogen	#700062
c-Myc	1:200	Santa Cruz Biotechnology	sc-40
CD36 (H-300)	1:200	Santa Cruz Biotechnology	sc-9154
CD47 (H-100)	1:200	Santa Cruz Biotechnology	sc-25773
VE-cadherin (F-8)	1:200	Santa Cruz Biotechnology	sc-9989
CTGF	1:300	Bio Vision	5553R
α-SMA (1A4)	1:200	Sigma-Aldrich	A2547
PECAM (M-20)	1:200	Santa Cruz Biotechnology	Sc-1506
GFP	1:500	Millipore	MAB2510

Online Table II.   qPCR primer sequences

rat *Gapdh*	forward 5'-AATGTATCCGTTGTGGATCTGAC-3'
	reverse 5'-TCTCTTGCTCTCAGTATCCTTGC -3'
rat *Itgav*	forward 5'- TGAGGATCTCTTCAACTCTACGC -3'
	reverse 5'- AAATACCAACACGGCCAGTAAC -3'
rat *Itgß1*	forward 5'- GAGACTCCAGACTGTCCTACTGG -3'
	reverse 5'- CACTTGGCATTCATTTTCTCCT -3'
rat *Itgß3*	forward 5'- AGGCCTCAAGTCTTGTGTGG -3'
	reverse 5'- TAGTGAAAGATTGCTCCTTCTGC -3'
rat *Fn1*	forward 5'- GAGTACATTGTCACCATCATTGC -3'
	reverse 5'- TGATTCTGTAATAGCGCACAGAG -3'
rat A*cta2*	forward 5'- GTCGCCATCAGGAACCTCGASAA -3'
	reverse 5'- CACCAGCAAAGCCCGCCTTACA -3'
rat *Myh11*	forward 5'- AAGACAGCAGCATCACGGGGA -3'
	reverse 5'- TGCCAAAGCGGGAGGAGTTGTC -3'
rat *Fbn1*	forward 5'- CCGGATGGAAAACCTTACCT -3'
	reverse 5'- GCAAGTGCACATGTTTGGTC -3'
rat *Eln*	forward 5'- GAGTTAGGGTCCCAGGTGCT -3'
	reverse 5'- CAGCTTTGGCAGCAGCTT -3'
rat *Lox*	forward 5'- TTGAGTCCCGGATGTTATGA -3'
	reverse 5'- CCAGGTAGCTGGGGTTTACA -3'
rat *Cpeb3*	forward 5'- TCTCCAATCAGCAGAGCTACATT -3'
	reverse 5'- TAGTACTGCAGACAGGTGACGTT -3'
rat *Tet3*	forward 5'- CGTCTGGGACTGAAGGAAGG -3'
	reverse 5'- CATCTTGTACAGGGGTAGCACAT -3'